International Journal of Computing and Digital Systems
ISSN (2210-142X)

Enhancing and Denoising Mammographic Images for Tumor Detection using Bivariate Shrinkage and Modified Morphological Transforms

Yen Thi Hoang Hua[1,3], Giang Hong Nguyen[1,3,4], Luong Bao Binh[2,3] and Dang Van Liet[1,3]

[1]*University of Science, Ho Chi Minh City, Vietnam*
[2]*Ho Chi Minh City University of Technology, Vietnam*
[3]*Vietnam National University Ho Chi Minh City, Vietnam*
[4]*Cao Thang Technical College, Ho Chi Minh City, Vietnam*

March 26, 2024

Abstract: Breast cancer stands as a prevalent concern for women worldwide. Mammography serves as the frontline defense for early detection, yet its low X-ray dosage often leads to suboptimal image quality. This study proposes a multi-step solution: (i) Image enhancement employs a two-step approach: denoising using bivariate shrinkage and a hybrid median filter based on stationary wavelet transform (SWT) to avoid shift variants, and it is combined with modified morphology operations including the background, a vignette image with the weighting function $1/R^2$. (ii) Segmentation utilizes the fast K-means algorithm with a straightforward technique to automatically determine the number of clusters and tumors within the segment containing the largest centroid. (iii) Classification employs an artificial neural network (ANN) model, based on statistical features extracted from SWT coefficients at different levels, for tumor classification to achieve reliable results. Utilizing data from the Mammographic Image Analysis Society (MIAS) database, the proposed method was tested on Gaussian noisy images, demonstrating superior performance compared to existing algorithms in detecting lesions. The segmentation achieves a high accuracy, 98.15% on average and a specificity of 99.56%. However, the ground truth occasionally extends beyond the tumor mass, resulting in a low sensitivity of 62.81%. Finally, classification is also performed using the ANN model giving an overall data accuracy of 96%.

Keywords: Breast Cancer, Mammogram, Stationary Wavelet Transform, Bivariate Shrinkage, Morphological Transform, Segmentation

1. INTRODUCTION

According to the World Health Organization (WHO), 2.3 million women were diagnosed with breast cancer in 2020, and 685,000 people lost their lives to the disease that year [1]. Breast cancer remains a significant global public health problem, impacting on numerous women and their families each year. The importance of early detection is widely recognized as a crucial element in improving patient outcomes and reducing mortality rates associated with breast, fibrous and glandular cancers.

One of the early detection methods for breast cancer is mammography, which involves taking X-ray specifically designed to examine the breast tissue. However, some mammograms may be noisy and have low contrast, making it difficult to distinguish between a tumor and dense breast tissue (fibrous and glandular) due to their almost equal brightness. Therefore, noise reduction and contrast enhancement are essential preliminary measures before image analysis. Various denoising methods have been proposed, with wavelet denoising being widely used. Here are some related works on denoising, enhancing and the detection of breast tumors in mammography image.

Amutha et al. (2011) [2] proposed a method for contrast enhancement and denoising of mammography images, using mathematical morphology for contrast enhancement and biorthogonal wavelet for denoising. The process involved splitting the image into low and high frequency components using a Gaussian low-pass filter, applying a mathematical morphology to the low-pass filtered part and an edge enhancement algorithm to the high-pass filtered part, and then combining these components to achieve contrast enhancement. Vikhe et al. (2016) [3] introduced a straightforward algorithm for enhancing and detecting masses in mammograms based on undecimated wavelet function-based denoising and adaptive thresholding technique. Fan et al. (2019) [4] presented an image denoising based on wavelet thresholding and Wiener filtering in the wavelet domain. Benhassine et al. (2021) [5] proposed an optimal image denoising method used for medical images using discrete wavelet transform (DWT). The obtained coefficients are thresholded using optimization algorithms. The performance of the method under different types of noise is determined by the criteria PSNR, MSE and SSIM. Kumar et al. (2012) [6] focused on enhancing mammographic images using a combination of enhancement using morphological filtering and denoising using biorthogonal

E-mail address: hthyen@hcmus.edu.vn, nguyenhonggiang@caothang.edu.vn, lbbinh@hcmut.edu.vn, dangvanliet@gmail.com

wavelet decomposition and thresholding. Sendur et al. (2002) [7] presented an image denoising method based on discrete wavelets called bivariate shrinkage. When denoising with the nonlinear threshold, the new shrinkage functions do not assume that the wavelet coefficients are independent, but rather that the threshold depends on the parent and child wavelet coefficients. Therefore, the image denoising is better than the result achieved by the traditional method. Yin et al. (2011) [8] discussed a novel image denoising algorithm based on modeling wavelet coefficients with an anisotropic bivariate Laplacian distribution function. The proposed anisotropic bivariate shrinkage approach was also extended to the DT-CWT domain to enhance the effectiveness of image denoising. The aforementioned studies demonstrated that noise reduction within the wavelet domain has traditionally treated components at different scales as independent, with the exception of the bivariate shrinkage method. The latter method takes into account the correlation between parent and child wavelet coefficients of the Discrete Wavelet Transform (DWT), but does not address contrast issues. This article serves two purposes: (i) consider mammographic image enhancement using denoising method based on stationary wavelet transform (SWT) with bivariate shrinkage functions and contrast enhancement using modified morphological operations and (ii): tumor detection using the fast K-means method and classification using an artificial neural network (ANN).

2. THEORETICAL BACKGROUND

A. Stationary Wavelet Transform

Wavelet analysis, valued for its time-frequency characteristics, finds significant use in image processing, particularly in denoising medical images like mammograms. Numerous research papers present this application [2-8]. The cornerstone of our denoising method is the use of the Stationary Wavelet Transform (SWT). Similar to Discrete Wavelet Transform (DWT), SWT decomposes an image into four components: approximate (A), vertical detail (V), horizontal detail (H) and diagonal detail (D) (Fig. 1). However, it does not perform down-sampling/up-sampling like DWT, but SWT performs upsampling of the coefficients of two low/high pass filters (Fig. 1a), so it maintains spatial localization and does not suffer from shift-variant problems. SWT handles edges and boundary effects more effectively than DWT, making it suitable for tasks such as image denoising and compression.

"À trous" is a common algorithm to calculate the Stationary Wavelet Transform (SWT) using a filter bank (h, g). The filters h are low-pass filters extracted from the scaling function, and the filters g are high-pass filters extracted from the wavelet function. For a 1-D signal, the algorithm produces a set of coefficients: w_j (high-pass filter) and c_j (low-pass filter) at scale j, given by:

$$c_j(k) = (\bar{h}^{j-1} * c_{j-1})[k] = \sum_l h[l] c_{j-1}[k + 2^{j-1} l] \quad (1)$$

$$w_j(k) = (\bar{g}^{j-1} * c_{j-1})[k] = \sum_l g[l] c_{j-1}[k + 2^{j-1} l] \quad (2)$$

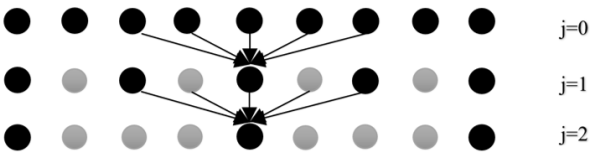

Black spot: filter coefficient; gray spot: zero padding
(a)

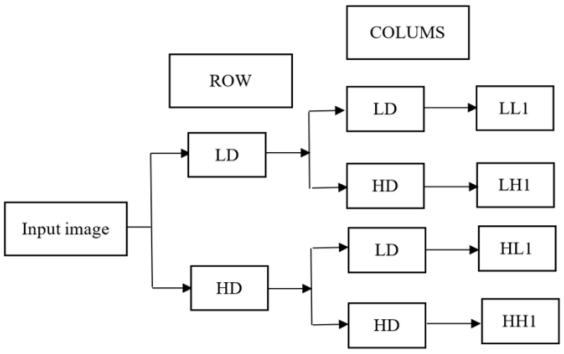

(b)

Figure 1. a) Padding 0 in the "À trous" filter, b) The flow-chart for single-scale SWT decomposition

where, $*$ denotes convolution and $h^j(k) = h(k)$ if $k/2^j$ is an interger and 0 for otherwise (Fig. 1a). So at each level, SWT coefficients have the same length as the original signal.

As a result, c_0 (reconstruction) can be expanded as the sum of the wavelet coefficients $w_j(k)$ and the final smoothing data c_N:

$$c_0(k) = c_N + \sum_{j=1}^{N} w_j(k). \quad (3)$$

This algorithm can be extended to images (2-d signals): approximation coefficient:

$$c_j[k, l] = (\bar{h}^{j-1} \bar{h}^{j-1} * c_{j-1})[k, l], \quad (4)$$

detail coefficient in horizontal direction:

$$w_j^1[k, l] = (\bar{g}^{j-1} \bar{h}^{j-1} * c_{j-1})[k, l], \quad (5)$$

detail coefficient in vertical direction:

$$w_j^2[k, l] = (\bar{h}^{j-1} \bar{g}^{j-1} * c_{j-1})[k, l], \quad (6)$$

detail coefficient in diagonal direction:

$$w_j^3[k, l] = (\bar{g}^{j-1} \bar{g}^{j-1} * c_{j-1})[k, l] \quad (7)$$

where, $hg * c$ denotes convolution first along the rows and the convolution along the columns [9] (Fig. 1b).

B. Bivariate Shrinkage

Bivariate shrinkage for wavelet is an approach employed to diminish the presence of noise in images by utilizing the correlation between wavelet coefficients at different scales [10].

Consider an image degraded by Gaussian noise,

$$g = x + \varepsilon \quad (8)$$

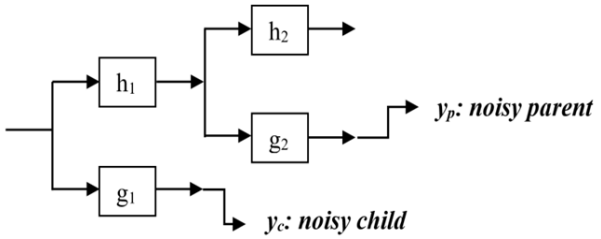

Figure 2. The analysis stage of bivariate shrinkage for wavelet decomposition

where ε is Gaussian noise, g is observation image and x is an noise-free image. The problem for denoising is to find x from g by some criteria such that x is as close to the original image as possible.
Levent Sendur and Ivan W. Selesnick [7], modified Bayesian estimation problem in the wavelet domain, has statistical dependence of the adjacent wavelet coefficients:

$$y = f + n \tag{9}$$

where, $\mathbf{y}(y_1, y_2)$, $\mathbf{f}(f_1, f_2)$, $\mathbf{n}(n_1, n_2)$ are respectively the wavelet coefficients of noisy image, free-noise image and noise; y_1 is the detail component of level k (child) and y_2 is the detail component of level $k+1$ (parent); these are two adjacent wavelet coefficients (Fig. 2).

According to Bayesian statistics, f is found from y through Maximum A Posteriori (MAP) Estimation:

$$\hat{\mathbf{f}}(y) = \underset{f}{argmax}\, P_{\mathbf{f}|\mathbf{y}}(\mathbf{f}|\mathbf{y}) \tag{10}$$

where, $P_{\mathbf{f}|\mathbf{y}}(\mathbf{f}|\mathbf{y})$ is the posterior probability (conditional probability of f while given y), given from prior probability through Bayes theorem:

$$P_{\mathbf{f}|\mathbf{y}}(\mathbf{f}|\mathbf{y}) = \frac{P_{\mathbf{y}|\mathbf{f}}(\mathbf{y}|\mathbf{f}).P_{\mathbf{f}}(\mathbf{f})}{P_{\mathbf{y}}(\mathbf{y})} \tag{11}$$

where, $P_{\mathbf{y}|\mathbf{f}}$ is the conditional probability of occurrence of y given f has occurred. $P_{\mathbf{y}}(\mathbf{y})$ is the probability of y and $P_{\mathbf{f}}(\mathbf{f})$ is the probability of f.
From that, Eq. (10) can be write:

$$\hat{\mathbf{f}}(y) = \underset{f}{argmax}\, [P_{\mathbf{n}}(\mathbf{y}-\mathbf{f}).P_{\mathbf{f}}(\mathbf{f})]. \tag{12}$$

According to Levent Sendur and Ivan W. Selesnick [7] this noise is iid-Gaussian noise with mean 0 and variance σ_n^2, noise pdf given by:

$$P_n(\mathbf{n}) = \frac{1}{2\pi\sigma_n^2} exp(-\frac{n_1^2+n_2^2}{2\sigma_n^2}) \tag{13}$$

$$= \frac{1}{2\pi\sigma_n^2} exp(-\frac{(y_1-f_1)^2+(y_2-f_2)^2}{2\sigma_n^2}). \tag{14}$$

For simplicity, based on the distribution of the wavelet coefficients, the model can be approximated by the bivariate probability density function $P_{\mathbf{f}}(\mathbf{f})$ given by [7]:

$$P_{\mathbf{f}}(\mathbf{f}) = \frac{3}{2\pi\sigma^2} exp(-\frac{\sqrt{3}}{\sigma}\sqrt{f_1^2+f_2^2}). \tag{15}$$

In this function, f_1 and f_2 are uncorrelated but not independent, with σ is marginal variance.

Substitute equations (14), (15) into (12), solutions of (10) (the MAP estimator or the joint shrinkage function) is given:

$$\hat{f_1} = \frac{\sqrt{y_1^2+y_2^2} - \frac{\sqrt{3}\sigma_n^2}{\sigma}}{\sqrt{y_1^2+y_2^2}}.y_1. \tag{16}$$

The result shows that the estimated value of f_1, depends not only on y_1 (child wavelet coefficient) but also on y_2 (parent wavelet coefficient), showing that the formula has a parent-child dependency; so, the accuracy will be better than soft thresholding.

C. Dual Morphological enhancement

Image enhancement involves improving the contrast of an image, often through denoising techniques like histogram stretching or equalization. The most common method is histogram equalization, which rearranges the histogram to increase contrast. However, when the resulting image is used to detect tumors, the tumor locations are different from the ground truth tumor locations. Therefore, in order to avoid the above disadvantages, this article uses morphological operations with top-hat and bottom-hat transforms. The top-hat transform is obtained as the disparity between the input image and its opening using a specific structural element, yielding an image that encompasses objects that are smaller than the structural elements and brighter for their surroundings. Conversely, the bottom-hat transform is derived from the difference between the input image and its closing, generating an image highlighting objects that are smaller than the structuring elements and darker for their surroundings. Consequently, combining the denoised image with the top-hat filtered image and then the bottom-hat filtered image is subtracted to obtain the contrast-enhanced image, which is called dual morphological enhancement [11].
- Top-hat transform:

$$T_{top-hat}(I) = I - (I \circ SE) \tag{17}$$

- Bottom-hat transform:

$$B_{bottom-hat}(I) = (I \bullet SE) - I \tag{18}$$

- Dual morphological enhancement:

$$I_{output} = I + T_{top-hat}(I) - B_{bottom-hat}(I) \tag{19}$$

where, I represents the original image, SE denotes the structuring element, $\circ$ the morphological opening operation and $\bullet$ the morphological closing operation.

D. K-means and Fast k-means

K-means is an unsupervised clustering algorithm that divides data into K different groups. First, let K be the number of clusters; each cluster randomly selects an initial centroid. Then do the following:
- Assignment step: Match each observation to its nearest center.
- Update step: Updates the centroids as their respective observable centers.
- Repeat these two steps until there are no further changes in the clusters. These are final clusters.

In mathematical terms, the K-means algorithm aims to minimize the objective function:

$$J = \sum_{i=1}^{m} \sum_{k=1}^{K} w_{ik} \|x^i - \mu_k\|^2 \quad (20)$$

where, $w_{ik} = 1$ for the data point x_i if it belongs to cluster k, otherwise, $w_{ik} = 0$; μ_k represents the centroid of cluster k.

The K-means method has a slow convergence rate; therefore, some authors have proposed the fast K-means method to accelerate convergence. According to Raied Salman et al. [12], the convergence rate is improved by dividing the distance calculation phase into two steps. Step 1, involves a fast distance calculation on a small subset data to determine the initial centroids. Step 2, calculates the exact distance over the entire data set using the initial centroids obtained in Step 1 to refine the centroids. The running time of this step is also minimized due to the lower number of iterations. Consequently, fast K-means converge quickly.

3. PROPOSED METHODOLOGY

Our proposed method includes three phases: preprocessing; noise reduction and contrast enhancement study; tumor extraction and classification. Details are described in the following sections.

A. Preprocessing

One of the goals of this article is image enhancement, which involves removing noise and improving contrast. Therefore, only markers, artifacts and pectoral muscle are eliminated in the preprocessing stage. To avoid performing numerous operations that later lead to positioning errors of the extracted tumor, these components are removed manually using Matlab software.

B. Denoising technique

Noise is a major factor affecting mammography. Therefore, denoising is required before segmenting the tumor. Fig. 3 shows the block diagram of the proposed denoising step for mammography images. In this proposed method, noise reduction in the wavelet domain is performed using a stationary wavelet transform. After decomposition, the detailed coefficients are denoised using the bivariate shrinkage method, which removes noise but preserves features, as described in Section 2-B, and the approximate components are smoothed using hybrid median filtering. Denoised images in the spatial domain are obtained using the inverse stationary wavelet transform. This article uses the four wavelet functions bior2.2, db4, sym2 and coeif2 to find the optimal wavelet function for noise reduction.

C. Contrast enhancement

Mammograms have low tumor-to-background contrast. Therefore, contrast enhancement using dual morphological enhancement (Section 2-C) is required. In this article, formula (19) is modified by applying a high-pass filter, which sharpens the edges more effectively than using the original image. The high-pass filtered image is obtained by subtracting the original image from the background image. The background image is typically

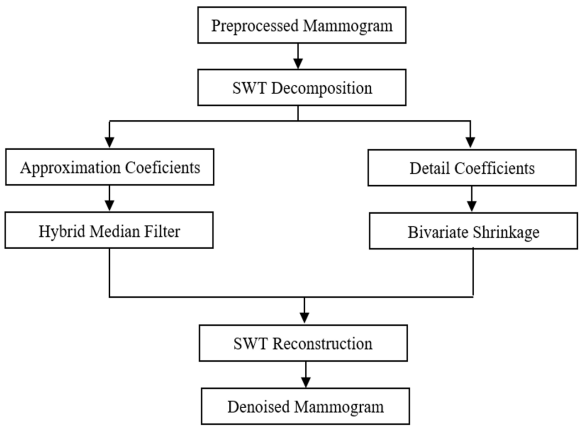

Figure 3. The block diagram for the proposed denoising methodology

obtained using average or low-pass Gaussian filtering. Here the background is a vignette image with a $1/R^2$ function, creating a bright center that fades toward the edges (vignette effect). This weighting function is multiplied by the original image to create the final background [13].

Wavelet fusion combines two denoising and contrast enhancing images to create a fused image that retains the most relevant features and information from the original data.

D. Image segmentation

In our proposed method, fast K-means is used for tumor extraction. The number of clusters corresponding to the number of main peaks of the image histogram was automatically selected by a program that detects these peaks. In cluster analysis, the cluster containing the tumor corresponds to the cluster with the maximum centroid value. In this cluster, extract 3 to 5 images, each image contains a tumor (counted from the largest tumor), and select the image as the segment containing the tumor. The source code for fast K-means is given by Ankit Dixit [14].

E. Image classification

Breast tumor classification aims to determine whether an image containing a mass is benign or malignant. In this article, the classification process consists of three steps: pre-processing, feature extraction and classification. The pre-processing step is designed to improve image quality through denoising and contrast enhancement, as examined in Sections 3-B and 3-C. This section introduces the steps of feature extraction and tumor classification.

Feature extraction:

Feature extraction is a transformative process that aimes to condense the input data to reduce complexity and highlight salient features and attributes facilitating effective classification. This is a crucial step in classification and is performed directly on the input image to extract low-level features or on transformed images to capture high-level features. There are various methods for feature extraction; in this article, some statistical features to measure central tendency, such as mean, root mean square (RMS), ratio of the mean, and several statistical features are used to evaluate the data's dispersion, such as standard deviation,

skewness, and kurtosis [15].
The above statistical features are applied to the approximation and detail coefficients of SWT with different levels to obtain high-level features. These features are enough to categorize the classes of the input image based on their characteristics.
Essentially, SWT is an extension of DWT but does not employ up-sampling and down-sampling of data. Therefore, the frequency bands of the approximation and detail coefficients in SWT vary from wide to narrow, corresponding to the levels from low to high. Therefore, the statistical features applied to the approximation and detail coefficients of SWT with different levels result in features at narrow and broad scales that captures sufficient properties of input classes for high classification accuracy. Statistical SWT features are contained in a feature matrix where the number of rows represents the instances and the number of columns represents the features.
Classifier:
In this article, Neural Network (ANN) - a well-known classifier - is used for classification tasks. The blocks of a Neural Network are node layers with an input layer, one or more hidden layers, and an output layer. Each node has a threshold and weight that are connected to other nodes. A node is activated and sends data to the following layer of the network when its output exceeds the threshold value. In contrast, no data is sent to the next layers of the network [16].

4. EXPERIMENTAL RESULTS

A. Data

The mammography images used in this study were provided by the well-known MIAS database [17]. This database contains 322 digitized mammograms with normal type and different types of abnormalities with their sizes and information about the structure of breast tissue. These features make it easier for users to evaluate their tumor detection and classification algorithms.
In this study, the authors used mammography image mdb001 from the dataset to determine optimal parameters for noise reduction by applying bivariate shrinkage combined with contrast enhancement using morphological operations. Breast tumor detection was performed using the fast K-means method on ten mammograms listed in Section 4-F and the results are evaluated using metrics such as accuracy, sensitivity and specificity. For the classification, an ANN classification model is created with 100 mamograms from the dataset, including 50 benign and 50 malignant mamograms.

B. Determine the optimal parameters for noise reduction

In this article, we will only investigate Gaussian noise reduction because this type of noise is consistenly present in images. The examined image is mdb001 (Fig. 4a), which has been corrupted by Gaussian noise and has a mean of 0 and $\sigma = 25$ (Fig. 4b). After pectoral muscle removal, the image undergoes bivariate shrinkage noise reduction through the use of a stationary wavelet transform, selecting wavelet functions from three different wavelet families, namely biorthogonal wavelet functions (bior2.2), orthogonal wavelet functions with asymmetric (db4), orthogonal wavelet functions with asymmetry with different length (sym2 (length 2N) and coif2 (length 6N)). Noise reduction results are evaluated using the Peak signal-to-noise ratio (PSNR) metric:

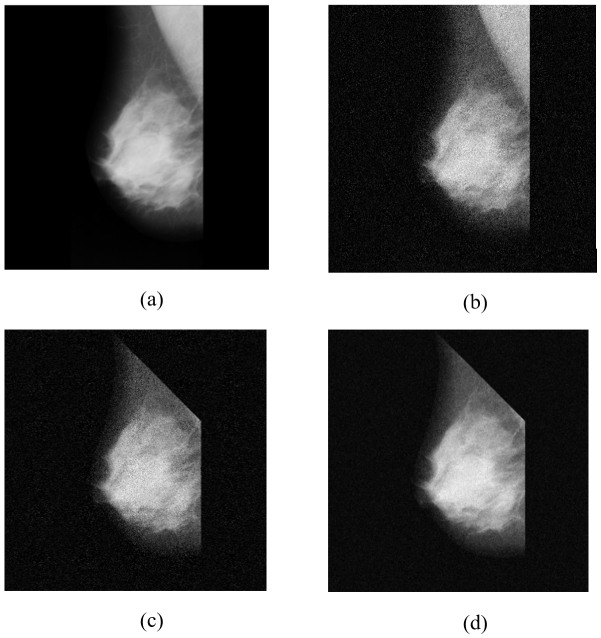

Figure 4. a) Original mammogram mdb001, b) Noisy mammogram with Gaussian noise ($\sigma = 25$), c) Preprocessed mammogram, d) Denoised and contrast enhancement mammogram using the proposed method.

TABLE I. PSNR values of the proposed denoising method with Gaussian noise $\sigma = 25$

Wavelet	bior2.2	db4	sym2	coif2
SWT level 1	26.38	27.29	**27.36**	27.28
SWT level 2	25.40	27.15	27.05	27.08
SWT level 3	25.30	27.34	27.22	27.27
SWT level 4	25.29	27.36	27.19	27.31

$$PSNR = 10log_{10}(\frac{MAX^2}{MSE}) \tag{21}$$

where, MAX is the maximum possible pixel value (255 for an 8-bit image) and MSE is the Mean Squared Error, which is calculated as the average of the squared differences between the original image and the processed image.
Table I shows the experimental results of image denoising for the Gaussian noisy image mdb001 ($\mu = 0, \sigma = 25$) by PSNR of four wavelet functions (bior2.2, db4, sym2 and coif2) at the first to fourth levels of SWT.
According to the results presented in Table I, the proposed denoising method using bivariate shrinkage with SWT produces the best results when the sym2 wavelet function at level 1 is used for comparison to other wavelet functions and the remaining levels. It can be observed that the sym2 wavelet function, a short-length filter suitable for noise reduction, along with level 1 decomposition, reveals that Gaussian noise with $\sigma = 25$ occupies approximately half of the high-frequency band of the image.

TABLE II. PSNR value of the proposed contrast enhancement method for mammogram contaminated with Gaussian noise σ = 25

Shape/Size	5	10	15	20
Disk	29.99	**30.04**	29.99	29.98
Square	29.99	30.02	29.97	29.99
Diamond	29.97	30.02	29.99	30.00

TABLE III. PSNR value of the proposed denoising method with different σ Gaussian noise.

Gaussian noise σ	Mean-Mean	Max-Min	Max-Max
5	**42.49**	41.46	39.28
10	**37.06**	36.02	33.63
15	**33.62**	32.60	30.10
20	**31.16**	30.13	27.62
25	**29.65**	28.25	25.75
30	**27.75**	26.68	24.19

C. Determine the optimal structuring element for contrast enhancement

After wavelet-based bivariate shrinkage for noise reduction, the study of contrast enhancement is carried out by using modified top-hat and bottom-hat transforms with multiple sets of structuring element shapes such as disk, square, diamond with radii in the range of 5, 10, 15, 20 are utilized [18].

Table II presents the experimental results of contrast enhancement for the mammogram mdb001 contaminated with Gaussian noisy ($\mu = 0, \sigma = 25$) by PSNR for three shapes of structuring elements: disk, square, diamond with different size: 5, 10, 15, 20.

According to the results of Table II, the disk shape of structural elements with size 10 is selected for contrast enhancement method.

D. Image for noise reduction and contrast enhancement

As described above, denoising using stationary wavelet-based bivariate shrinkage with sym2 wavelet function at the first level and the contrast enhancement using modified morphological operations with the disk shape in size 10 of structural elements achieves the best outcome. Therefore, to achieve both denoising and improved contrast, these two results are fused together using wavelet based image fusion techniques, for three cases mean-mean, max-min and max-max are performed. The results are presented in the Table III.

With varying standard deviation of Gaussian noise, the Mean-Mean method yields the optimal results as chosen in this article (Fig. 4d).

E. Compare the denoising results with other outcomes

In order to validate the above comment, the results are compared with the results of other thresholding methods in the article of [5] such as VisuShrink, Feed-forward denoising convolutional neural networks (DnCNN) and Benhassine et al. method [3] on the mdb001 mammogram with Gaussian noise using different standard deviations of 5, 10, 20 and 30, respectively. The results are shown in Table IV.

The value of PSNR for our proposed method is higher than all other enhancement techniques indicating better quality.

F. Tumor detection

The mammography enhancement (denoising and contrast enhancement) is then subjected to breast tumor detection using the fast K-means method. In this method, the breast tumor located in the segment with the maximum centroid value is extracted and smoothed using morphological operations.

In these experimental results, ten mammograms from the mini-MIAS database, representing five classes of abnormality, Circular (CIRC) mdb001 and mdb028, Miscellaneous (MISC) mdb063 and mdb058, Asymmetrical (ASYM) mdb104 and mdb111, Architectural Distortion (ARCH) mdb165 and mdb117, and Spiculated (SPIC) mdb198 and mdb184 were used to detect tumors because each class of abnormalities may have different characteristics. In the mini-MIAS database, each image provides ground truth for tumors. It is not represented in the actual shape but as a circle (with center and radius). Therefore, we ovelay the extracted breast tumor with a black circle representing the ground truth (provided by MIAS) on the original image to visualize the accuracy. To calculate the accuracy of the extracted tumor compared to the ground truth, the proposed method's extracted tumor is analyzed using the 'regionprops' function in Matlab to obtain its center coordinates, perimeter, area, and major and minor axes.. The radius is calculated as the average of the major and minor axes of the tumor and the extracted circle which is represented by the white shaded area in the mammogram.

Figures 5 and 6 are the segmentation results of two CIRC lesion mammograms. Circular lesions can vary in size but tend to be relatively symmetrical and often appear as a well-circumscribed mass with uniform density throughout the lesion. Through visualization and accuracy result, it shows that the proposed method achieves good sensitivity in these cases.

Figures 7 and 8 illustrate the segmentation results of two mammograms containing MISC lesions. The miscellaneous category is a catch-all for lesions that do not fit into the other categories; their shapes, edges, and internal density can vary greatly, making diagnosis more difficult. For example, in image mdb063, the result is achieved well, but for image mdb058, the result does not match the ground truth.

Figures 9 and 10 are the segmentation results of two mammograms containing ASYM lesions. These lesions are characterized by irregular shapes, lacking the symmetry typically seen in normal breast tissue, and may exhibit variations in density within the same lesion. The algorithm performs well for ASYM lesions due to the presence of significant gray level features.

Figures 11 and 12 display the segmentation results of two mammograms containing ARCH lesions. Architecturally distorted lesions typically have irregular edges that blend into the surrounding tissue, making them difficult to discern. Additionally, the internal density of these lesions can vary within the distortion and extend over a broader area. These characteristics limit the effectiveness of segmentation results based on the proposed method, leading to a high number of false positives.

TABLE IV. The PSNR of four methods with different standard deviations Gaussian noise

Gaussian noise σ	VisuShrink	DnCNN	Benhassine [5]	Proposed Method
5	38.48	39.05	40.76	**42.49**
10	33.78	31.71	35.53	**37.06**
20	29.57	25.53	30.25	**31.16**
30	26.83	22.15	27.15	**27.75**

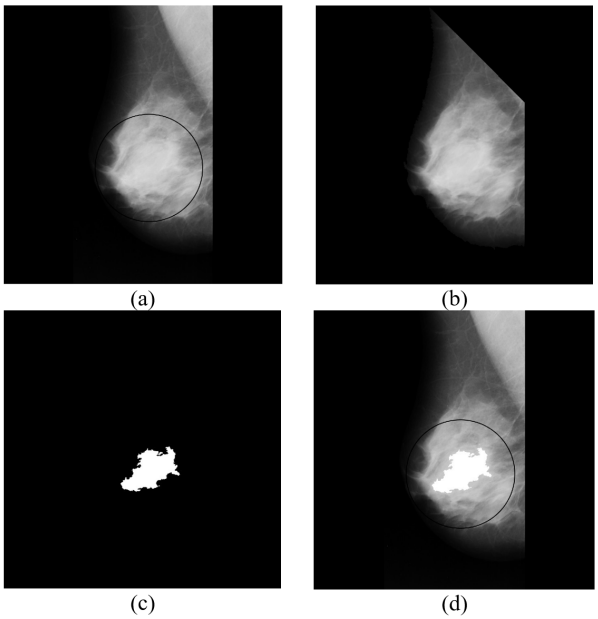

Figure 5. Result of CIRC lesion: a) Original mammogram mdb001 with ground truth (the black circled region contains the lesion), b) Processed mammogram by the proposed method, c) Final segmented tumor mass by fast K-means method, d) Output image (black circle: ground truth, whiteshaded area: proposed method).

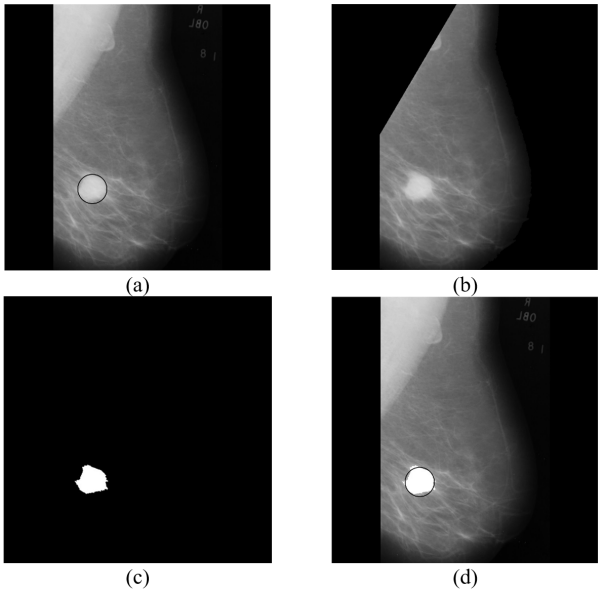

Figure 6. Result of CIRC lesion: a) Original mammogram mdb028, b) Processed mammogram, c) Final segmented tumor, d) Output image.

Spiculated lesions are characterized by linear or spiculated shapes, resembling spikes radiating from a central point. Their borders are typically irregular and exhibit variations in density within the lesion. Figures 13 and 14 illustrate the segmentation results of two mammograms containing SPIC lesions. The algorithm performs well for these types of lesions.

Through the tumor extraction results of ten mammograms and the corresponding ground truth; the true positive (TP), true negative (TN), false positive (FP) and false negative (FN) are evaluated to determine performance metrics such as:

$$Accuracy\ (Acc) = \frac{TP + TN}{TP + TN + FP + FN} \tag{22}$$

$$Sensitivity\ (Sen) = \frac{TP}{TP + FN} \tag{23}$$

$$Specificity\ (Spec) = \frac{TP}{TP + FP} \tag{24}$$

The results are shown in Table V.

According to the results in Table V, the proposed method achieves an average accuracy of 98.15% and specificity of 99.56%. Because the ground truth is represented by a circle that can extend beyond the tumor mass, the FN

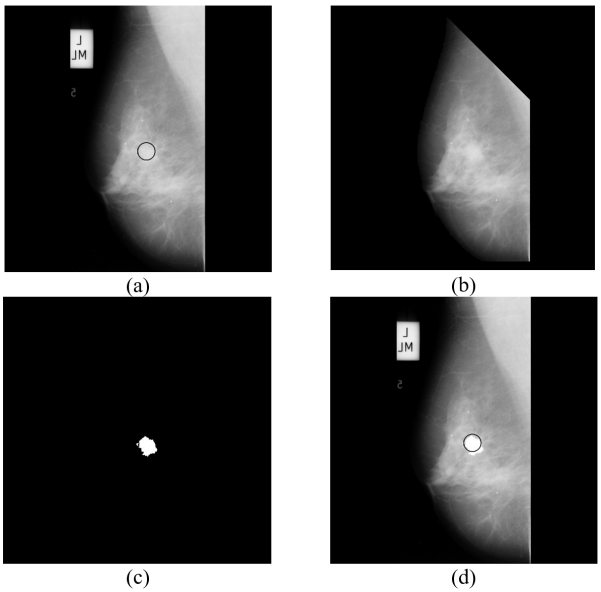

Figure 7. Result of MISC lesion: a) Original mammogram mdb063, b) Processed mammogram, c) Final segmented tumor, d) Output image.

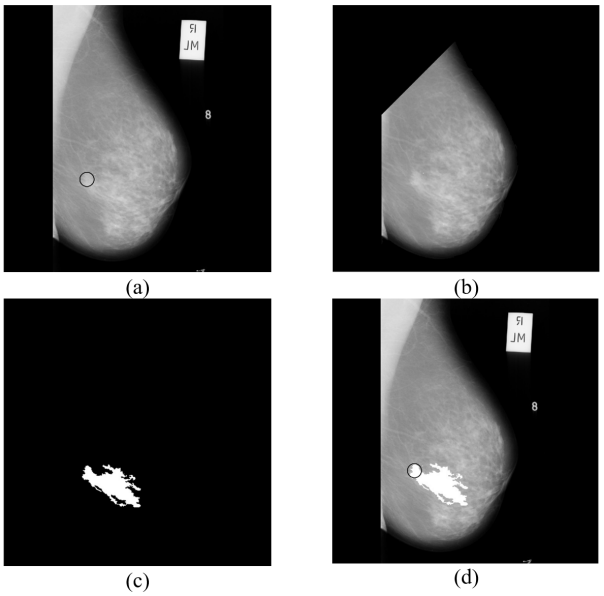

Figure 8. Result of MISC lesion: a) Original mammogram mdb058, b) Processed mammogram, c) Final segmented tumor, d) Output image.

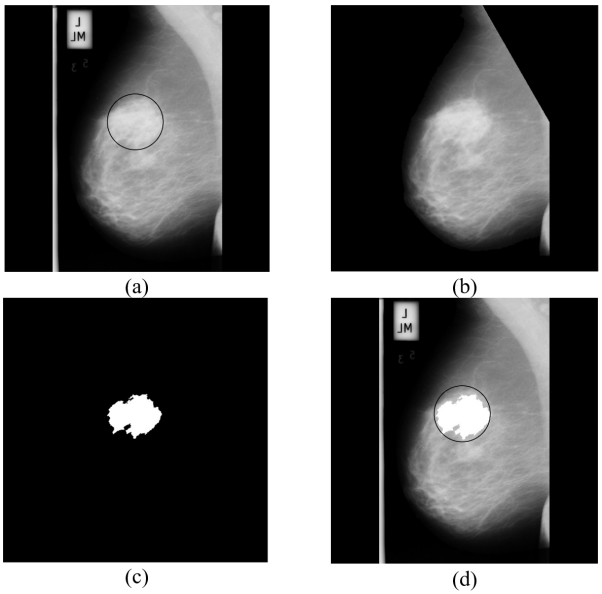

Figure 10. Result of ASYM lesion: a) Original mammogram mdb111, b) Processed mammogram, c) Final segmented tumor, d) Output image.

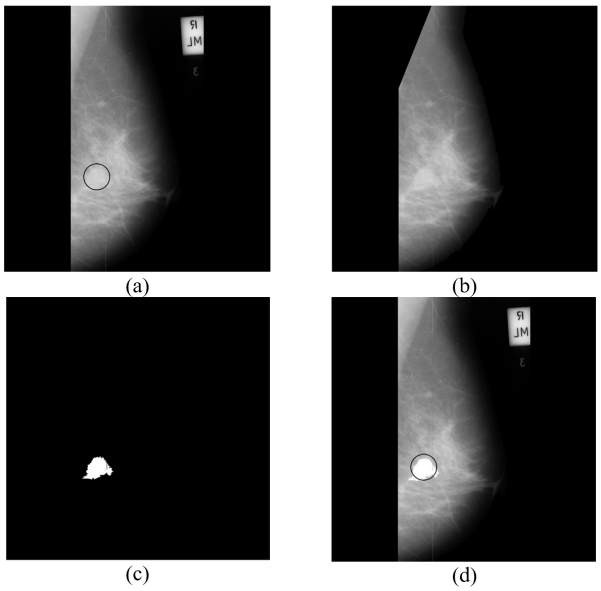

Figure 9. Result of ASYM lesion: a) Original mammogram mdb104, b) Processed mammogram, c) Final segmented tumor, d) Output image.

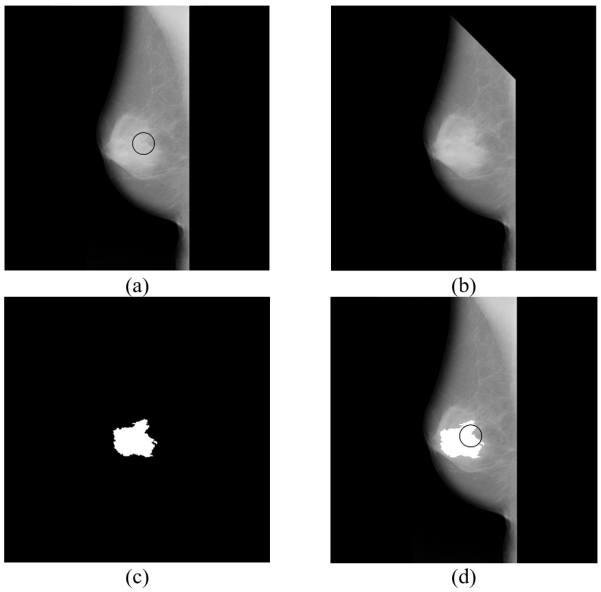

Figure 11. Result of ARCH lesion: a) Original mammogram mdb165, b) Processed mammogram, c) Final segmented tumor, d) Output image.

is relatively high, resulting in a low sensitivity of only 62.81%.

G. Classification results

Data were extracted from the mini-MIAS dataset, from which 50 benign and 50 malignant tumor images were selected to calculate six statistical features: the mean absolute value, the standard deviation, the skewness, the kurtosis, the RMS power, and the ratio the mean absolute values of two consecutive subbands of the approximation and detail coefficients of the SWT, from level 1 to level 8 using the 'db4' wavelet function. Therefore, each image is represented by 95 features recorded in a SWT feature matrix of size 100x96. Columns 1 to 95 represent the features, and column 96 represents the label of the image. This matrix is divided into two sets: the training set (80%) and the test set (20%), which are used to build a classification model based on the ANN classifier.

An ANN classifier with 90 hidden layers was created using the 'train' function in MATLAB. The 'trainlm' function was used to train the network with the training set described above. The results showed that the model performed well, with training accuracy of 100%, testing accuracy of 75%, and all data accuracy of 96% (Fig. 15). The relatively low accuracy of the test data indicates the need to select additional data and perhaps include some additional statistical features.

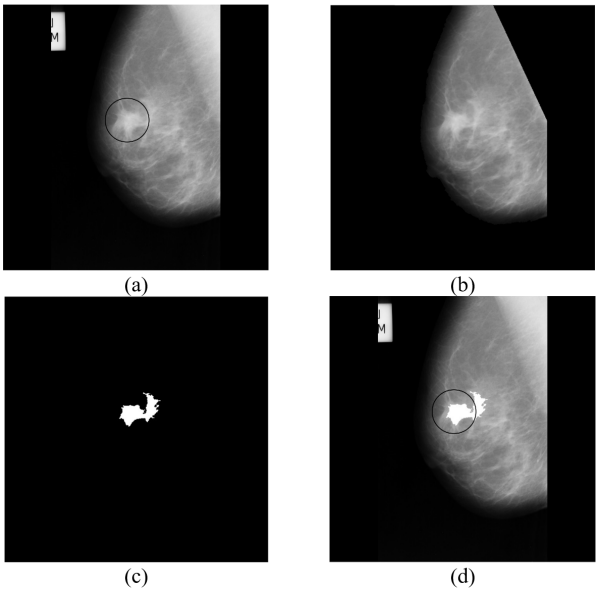

Figure 12. Result of ARCH lesion: a) Original mammogram mdb117, b) Processed mammogram, c) Final segmented tumor, d) Output image.

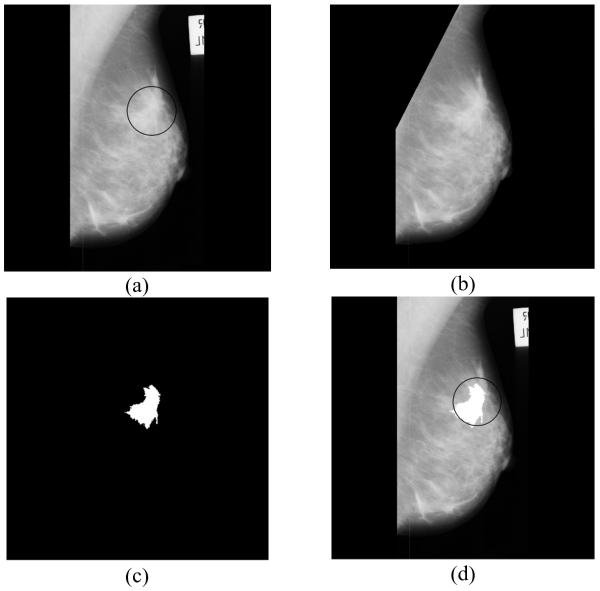

Figure 13. Result of SPIC lesion: a) Original mammogram mdb198, b) Processed mammogram, c) Final segmented tumor, d) Output image.

However, in this article, the model is used to classify images in the image segmentation section. The results are presented in Table VI.

Comparing the experimental results with the ground truth of the mammograms database, in out of ten diagnosed images, nine images were predicted accurately and one image reveals a misidentification in the diagnostic outcome, where a benign tumor in image mdb198 is incorrectly identified as a malignant tumor. It is obvious that this is a good result with the proposed method.

5. CONCLUSION

Mammography is the leading technology for early breast cancer detection and breast tumor analysis. The

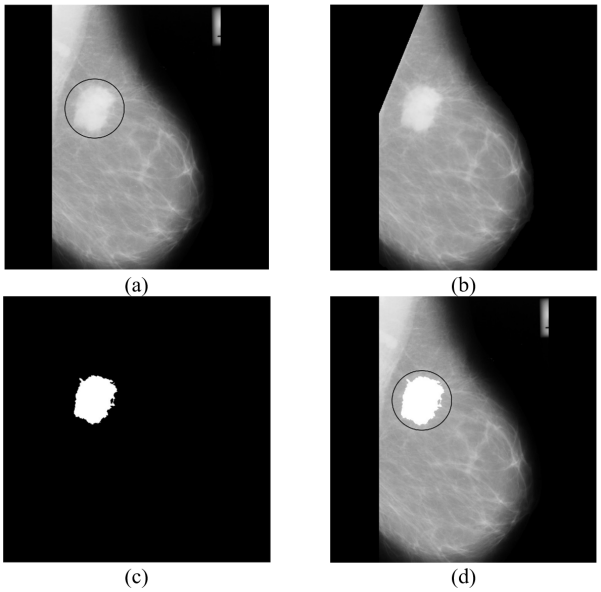

Figure 14. Result of SPIC lesion: a) Original mammogram mdb184, b) Processed mammogram, c) Final segmented tumor, d) Output image.

TABLE V. The results of evaluation metrics in ten experimental mammograms

Images	Acc (%)	Sen (%)	Spec (%)
mdb001	90.79	34.61	100.00
mdb028	99.86	93.22	99.86
mdb063	99.82	76.84	99.84
mdb058	97.56	2.15	97.74
mdb104	99.77	84.85	99.87
mdb111	99.16	86.11	100.00
mdb165	98.71	42.97	98.74
mdb117	98.51	58.56	99.57
mdb198	98.83	71.93	99.94
mdb184	98.53	76.83	100.00
Average	98.15	62.81	99.56

TABLE VI. The results of classification in ten experimental mammograms

Images	Ground truth	Method
mdb001	Benign	Benign
mdb028	Malignant	Malignant
mdb063	Benign	Benign
mdb058	Malignant	Malignant
mdb104	Benign	Benign
mdb111	Malignant	Malignant
mdb165	Benign	Benign
mdb117	Malignant	Malignant
mdb198	Benign	Malignant
mdb184	Malignant	Malignant

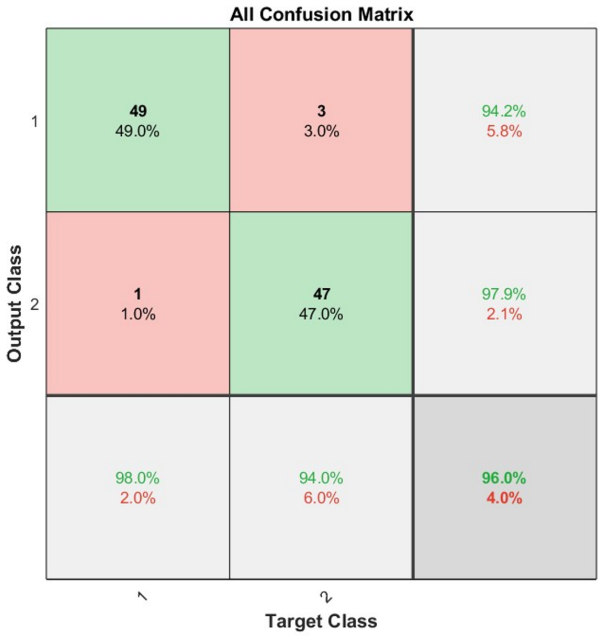

Figure 15. All confusion matrix of the model

proposed method is intended to aid radiologists in interpreting images and contribute to the overall fight against this formidable disease. By integrating computational techniques, breast cancer screening can achieve improved accuracy and reduced false positives.

The proposed method demonstrates its effectiveness in three key steps of medical analysis: image enhancement, segmentation, and classification. This significantly improves the accuracy of disease diagnosis, as shown by the following experimental results:

(a) Shift invariance is crucial in image denoising. The lack of shift invariance implies that small shifts in the input signal lead to significant fluctuations in the energy distribution between the transform coefficients at different scales and are therefore not suitable for denoising. Then, SWT-based denoising method with bivariate shrinkage and hybrid median filter provides a robust solution for image denoising.

(b) The vignette effect, when used with modified morphological operations, can increase the focus on details in the central area, thereby significantly increasing the contrast between objects and their surrounding area and thus improves segmentation.

(c) The choice of clustering fast K-means algorithms by automaticcally binning the histogram distribution makes this method more advantageous in the segmentation process.

(d) Feature extractions from the wavelet coefficients of SWT from level 1 to level 8 show that the features extracted at different scales correspond to the characteristics of the image in frequency ranges from wide to narrow. This ensures that feature extractions are sufficient for effective classification even when there are not many instances.

This article calculates noise reduction for image enhancement and statistical feature extraction for classification based on SWT coefficients. In particular, the K-means algorithm is used in the segmentation step. Therefore, segmentation using SWT and the extraction of other features in addition to statistical features for classification are the tasks of the future.

ACKNOWLEDGMENT

This research is funded by Vietnam National University, Ho Chi Minh City (VNU-HCM) under grant number C2022-18-08.

REFERENCES

[1] H. Sung et al., "Globalcancer statistics 2020: Globocan estimates of incidence and mortality worldwide for 36 cancers in 185 countries," *CA: A Cancer Journal for Clinicians*, vol. 71(3), pp. 209–249, 2020.

[2] J. Amutha and N. Sundararajan, "Mammographic image enhancement using modified mathematical morphology and bi-orthogonal wavelet," *International Journal of Computer Applications*, vol. 17(7), pp. 22–25, 2011.

[3] P. S. Vikhe and V. R. Thool, "Mass detection in mammographic images using wavelet processing and adaptive threshold technique," *J Med Syst*, vol. 40(82), pp. 1–11, 2016.

[4] W. Fan and W. Xiao, "Image denoising based on wavelet thresholding and wiener filtering in the wavelet domain," *The Journal of Engineering*, vol. 2019(19), pp. 6012–6015, 2019.

[5] N. E. Benhassine, A. Boukaache, and D. Boudjehem, "Threshold selection for wavelet-based denoising of medical images: a review," *International Journal of Biomedical Engineering and Technology*, vol. 36(2), pp. 94–109, 2021.

[6] H. Kumar, R. Babu, and A. B. P, "Enhancement of mammographic images using morphology and wavelet transform," *International Journal of Computer Technology & Applications*, vol. 3(1), pp. 192–198, 2012.

[7] L. Sendur and I. W. Selesnick, "Bivariate shrinkage functions for wavelet-based denoising exploiting interscale dependency," *IEEE Transactions on Signal Processing*, vol. 50(11), pp. 2744–2756, 2002.

[8] S. Yin, H. Li, and et al, "Anisotropic bivariate shrinkage function for wavelet-based image denoising. signal processing," *Signal Processing*, vol. 91(8), pp. 2078–2090, 2011.

[9] S. Jean-Luc, F. Jalal, and M. Fionn, "The undecimated wavelet decomposition and its reconstruction," *IEEE Transactions on Image Processing*, vol. 16(2), 2007.

[10] D. Donoho, "Image denoising using scale shrinkage and wavelet transform," *IEEE Transactions on Image Processing*, vol. 4, pp. 57–69, 1995.

[11] R. Anitha and C. Chandrasekar, "A dual stage adaptive thresholding (DuSAT) for automatic mass detection in mammograms," *Computer methods and programs in biomedicine*, vol. 138, pp. 93–104, 2017.

[12] R. Salman, V. Kecman, and Y. Li, "Two-stage clustering with k-means algorithm," *Engineering in Agriculture, Environment and Food*, vol. 11(3), pp. 110–125, 2018.

[13] MathWorks, "Increase filter strength radially outward," *Matlab Documentation*.

[14] A. Dixit, "Fast kmeans algorithm code (https://au.mathworks.com/matlabcentral/fileexchange/44598-fast-kmeans-algorithm-code)," *Matlab Central File Exchange*, 2023.

[15] B. Esmaeil, A. Arnaout, and et al, "A statistical feature-based approach for operations recognition in drilling time series," *8th International Conference on Intelligent Computing, ICIC 2012*, vol. 7389, pp. 460–466, 2012.

[16] S. Kaymak, A. Helwan, and D. U. Ozsahin, "Breast cancer image classification using artificial neural networks," *Procedia Computer Science*, vol. 120, pp. 126–131, 2017.

[17] M. I. A. Society, "Mini mammography database. retrieved from http://www.wiau.man.ac.uk/ services/miasimia-smini.htm," 2008.

[18] Y. Hua, G. Nguyen, and L. Dang, "Detection of abnormalities in mammograms by thresholding based on wavelet transform and morphological operation," *Intelligent Systems and Networks. ICISN 2023. Lecture Notes in Networks and Systems*, vol. 752, pp. 496–506, 2023.

Giang Hong Nguyen received the M.Sc. degree in Radio Physics and Electronics (Speciality of appied physics) from the University of Science,Vietnam National University, Ho Chi Minh City, Vietnam in 2021. He is currently PhD student of Engineering Physics fromUniversity of Science, VNU HCM, Vietnam. His area of research interests are Signal and Image Processing, Machine Learning.

LUONG Bao Binh earned his Ph.D. in Geodesy in 2011 from Graz University of Technology, Austria. Currently, he serves as the Chair of the Geomatics Engineering Department at Ho Chi Minh City University of Technology. His research focuses on geodesy and geoid computation, as well as LiDAR and image processing for UAV and mobile mapping systems.

Yen Thi Hoang Hua received her M.Sc. degree of Physics in 2007 and currently enrolled in a doctoral program of Engineering Physics from the University of Science-Vietnam National University, Ho Chi Minh City. She is a Lecturer at Department of Physics and Computer Science, Faculty of Physics and Engineering Physics, University of Science-VNU HCM, Vietnam. Her area of interest includes Signal and Image Processing, Machine Learning, Deep Learning. Her email is hthyen@hcmus.edu.vn

Dang Van Liet received his Ph.D. in Mathematics – Physics from the University of Ho Chi Minh City (now Vietnam National University, Ho Chi Minh City) in 1995. He is an invited Associate Professor at the Dept. Physics – Computer Science at the University of Science (Vietnam National University, Ho Chi Minh City). His areas of interest are Signal and Image Processing, Machine Learning, Gravity and Magnetic data analysis. His email is dangvanliet@gmail.com